N85-22480

DIRECT MEASUREMENTS OF SEVERE SPACECRAFT CHARGING IN AURORAL IONOSPHERE

W. J. Burke, D. A. Hardy, F. J. Rich, and A. G. Rubin
Air Force Geophysics Laboratory
Hanscom Air Force Base, Massachusetts 01731

M. F. Tautz
Radex Inc.
Carlisle, Massachusetts 01741

N. A. Saflekos* and H. C. Yeh
Boston College
Chestnut Hill, Massachusetts 02167

Due to limitations of methods commonly used to detect particles and plasmas few examples of spacecraft in the ionosphere charging beyond a few volts appear in the literature. This impasse has been overcome with the launch of the DMSP/F6 satellite. It was equipped with up-looking detectors to measure 20 point spectra of precipitating ions and electrons with energies between 30 eV and 30 KeV, once per second. A generous geometric factor for the ion detector allows the application of a technique regularly used to identify the degree of charging for satellites at geostationary orbit. The Liouville Theorem can be used to show that a spacecraft charged, to say, -100 V, will measure no positive ions in energy channels < 100 eV. Because of the acceleration of cold, ionospheric ions by the spacecraft potential a large count rate should be seen in an energy channel centered near 100 V. A preliminary search of early DMSP measurements shows that such charging peaks frequently appear in the vicinity of intense inverted-V structures. An example that closely approximates the "worst case" charging environments derived from previous DMSP missions, with only electron measurements available has been examined. In this case, with the satellite in darkness, peak electron fluxes occurred at energies of 10 keV and charging peaks were observed in ion energy channels up to ~65 eV. The fact that the spacecraft was charged was verified using the SSIE thermal plasma probe on the same vehicle. Calculations indicate that dielectric surfaces in the wake side of the vehicle charge to many times this number.

* Present address: Southwest Research Institute, Space Physics Section, San Antonio, TX 78284.

INTRODUCTION

In this symposium we are addressing questions concerning how large space structures in polar orbit will interact with auroral environments. Because spacecraft charging at ionospheric attitudes does not seriously threaten the operation of today's relatively small polar satellites the subject of environment interactions has not received the widespread attention given to it at geostationary altitude. As a matter of economics it is desireable for us to apply as much as possible of what we have learned about spacecraft interactions at geostationary orbit to low earth orbits. Economics, however, must not blind us to real differences between the two problems.

The environment at auroral latitudes in the ionosphere differs from that encountered at geostationary altitude in at least two major aspects.

(1)   There is a large reservoir of high-density, cold plasma which tends to mitigate charging effects by providing a large source of charged particles from which neutralizing currents maybe drawn. However, since Debye lengths in the ionosphere are measured in centimeters as opposed to hundreds of meters at geostationary altitude effective current collecting areas may be severely limited. Significant wake effects behind large structures will introduce new problems with differential charging.

(2)   Between the magnetic equator and the ionosphere, auroral electrons frequently undergo field-aligned accelerations of several kilovolts (ref. 1). The degree to which auroral, as opposed to plasma sheet, electrons deviate from isotropy is a complex function of the electron's energy and the potential distribution along magnetic field lines (ref. 2). In such environments, fluxes of energetic protons are usually below the levels of instrumentation sensitivity (refs. 3 and 4).

It is anticipated that polar-orbiting shuttles will encounter the most severe charging environments in the vicinity of westward travelling surges and near inverted-V structures. Westward travelling surges occur in the midnight sector during the expansion phases of substorms. Substorm onsets are frequently marked by the sudden brightening of the equatorward-most arc (ref. 5). This is followed by a bulging and rapid poleward expansion of active arcs in the midnight sector (ref. 6). For observers on the ground in the evening sector the bulge appears on the eastward end of arcs and moves quickly toward the western horizon. Using DMSP satellite imagery and electron flux measurements Meng and coworkers (ref. 7) constructed a composite morphology of westward travelling surges shown in Figure 1. Bright arcs emanate to the west (A) and to the east from the equatorward and poleward edges of the bulge region, respectively. A myriad of arc-like structures are embedded in the bulge region (C), while nonuniform diffuse auroral precipitation (D) is found to the east of the bulge and equatorward of the B arc.

Differential spectra typical of downcoming electrons in the vicinity of surges are shown on the left side of Figure 1. In region A, to the west (evening side) of the bulge, spectra are similar to those measured over quiet-time arcs. However, the "monoenergetic beams" shift to higher than quiet-time values. This indicates that stronger field-aligned potentials occur during substorm periods. In the region of the poleward arc (region B) two spectral types are measured. One has a shape similar to that found in the diffuse aurora (D) but with lower mean energy. The second spectral type is characterized by electrons with energies of 100 eV and differential flux levels of $10^{11}/cm^2$ sec sr keV. The spectral shapes indicate that field-aligned accelerations in regions B and D are not significant. Within region C electron spectra are relatively flat, sometimes out to the high-energy, measuring limit of

DMSP spectrometers. If, as suggested by the "worst-case" study of SCATHA's environment (ref. 8), severe charging most strongly correlates with fluxes of electrons with energies in the several tens-of-keV regime, then region C electrons may present the most severe charging environment for polar-orbiting shuttles.

Hazards due to spacecraft charging of large space structures should also occur in "inverted-V" events. The term inverted-V was first used to describe structures that appear in energy-time spectrograms from polar orbiting satellites (ref. 3). In these structures the mean energy of precipitating electrons rises from a few hundred eV to several keV then returns to a few hundred eV. Often the electrons have Maxwellian distributions characterized by a mean thermal energy E_0 that have been accelerated through a field-aligned potential drop ϕ_0 (ref. 9). In traversing the inverted-V, ϕ_0 increases to some maximum value then decreases. In the evening sector ϕ_0 can rise to over 10 kV. The danger posed by inverted-V precipitation is more ubiquitous than westward travelling surges. Lin and Hoffman (ref. 2) showed that inverted-V events occur in all MLT sectors except in the dayside auroral gap (ref. 10).

To date, all investigations of inverted-V structures report no measurable fluxes of precipitating protons. This limitation more likely reflects on the sensitivity of proton detectors rather than on a real absence of proton fluxes. In the plasma sheet protons have mean thermal energies that are about five times those of electrons. Some protons in the high energy tail of these distriutions should be sufficiently energetic to overcome the ϕ_0 potential barrier and reach the ionosphere.

Herein lies a serious verification problem for modelers of low-earth orbit spacecraft charging. It is rather easy to specify the "worst charging environment" (ref. 11). However, the relatively small geometric factors on positive ion detectors flown to date on polar satellites have not allowed us to use the straight-forward methods used at geostationary altitudes (ref. 8) for measuring satellite potentials in excess of a few volts. In only one case, as INJUN-5 passed through an intense inverted-V, has a large satellite potential been measured (ref. 12). In this case only an upper bound of -28V could be directly assigned.

The purpose of this report is to provide information for interaction-modelers on the capabilities of a new generation of charged particle spectrometers now flown on DMSP (Defense Meteorological Satellite Program) satellites. These detectors, which are sensitive to downcoming, positive ions with energies greater than 30 eV, allow the direct measurements of satellite potentials less than -30V. The following section describes the plasma and particle instrumentation on the recently launched DMSP/F6 satellite. We then present a detailed analysis of measurements taken as the satellite passed through an intense, inverted-V structure in the midnight sector on 10 January 1983. The discussion section compares observational measurements of the satellite potential with the predictions of a small-satellite charging model.

INSTRUMENTATION

DMSP satellites are three axis stabilized and fly in sun-synchronous, circular polar orbit at an altitude of 840 km. Their orbital periods and inclinations are are 101 minutes and 98.75°, respectively. DMSP/F6 was launched in late December 1982 into an orbit near the dawn-dusk meridian with an ascending mode of 0612 LT. The two sets of detectors of interest here were designed to monitor variations in the topside thermal plasma and in the flux of precipitating charged particles.

The thermal plasma detector (ref. 13, 14), known as the Special Sensor for Ions and Electrons (SSIE) consists of a spherical Langmuir probe and a planar, retarding potential analyzer (RPA). The Langmuir probe consists of a 1.75" diameter collector surrounded by a concentric, wire-mesh grid of 2.25" diameter. It is mounted at the end of a 2.5' rigid boom. The sensor operates in 2 modes. In the first mode the grid bias is held at a fixed level determined by ground command. In the second mode the voltage of the grid with respect to satellite ground is swept to determine the thermal electron density and temperature. The mode 2 voltage sweep occurs every 64 s and lasts for 10 s. To ensure that all electrons passing through the grid are collected the collector is always held at a potential of 20 V above that of the grid. During Mode 1 operations on 10 January 1983 the grid-bias was fixed at +7.8 V with respect to the spacecraft frame potential.

The thermal ion detector is a retarding potential analyzer (RPA) that consists of a collector, a supressor grid, a swept grid and an aperture grid. The aperture grid is circular with a diameter of 1.0". This sensor is mounted 3/4 of the way up the 2.5' boom with an outward surface normal facing in the direction of the satellite velocity. The RPA also operates in two modes. In Mode 1 the retarding grid is fixed at satellite potential plus a bias potential of 6.3V. In Mode 2 the retarding grid is swept from -5 V to 12 V, every 64 s. From the shapes of the current-voltage characteristics obtained during Mode 2 sweeps it is possible to determine the ion densities, temperatures and relative mass concentrations. Complete descriptions of the SSIE instruments and the methods of data reduction and analysis have been written by Smiddy and co-workers (ref. 13) and by Rich and co-workers (ref. 14).

The energetic particle detector on DMSP/F6 are designed to measure the flux of downcoming electrons and positive ions in 20 energy channels, logrithmically spaced between 30 eV and 30 keV. Both the electron and ion detectors consist of two curved plate electrostatic analyzers. The aperatures of the analyzers always face toward local vertical. Thus, at auroral and polar-cap latitudes they detect precipitating rather than backscattered or trapped particles. One set of analyzers covers the energy range 30 eV to 1 keV has a geometric factor of 4×10^{-4} cm^2-sr for electrons and 2×10^{-2} for ions. In both cases $\Delta E/E$ is 13%. The other set of analyzers measures the flux levels over the 1 to 30 keV range. The geometric factor for these electron and ion detectors is 10^{-3} cm^2-sr with $\Delta E/E = 10$%. These large geometric factors ensure statistically significant count rates in the auroral oval.

OBSERVATIONS

During the period of interest on 10 January 1983, DMSP was in darkness crossing the midnight sector of the northern auroral oval from dawn to dusk. Simultaneous measurements from the imager on F6 and ground magnetograms are not available at this time. In general, however, the period may be characterized as one of magnetic quieting. Although Kp was 2+ at the time of the overpass, 10 January was the most disturbed day of the month with $\Sigma Kp = 39$.

Measurements from the energetic electron and ion spectrometers are presented in Figures 2 and 3, respectively. The format for data presentation is the same in both figures. Plotted as functions of UT, geomagnetic latitude, and magnetic local time are the particle's average energies (top panel), the directional energy fluxes (middle panel) and number fluxes (bottom panel). Attention is directed toward the one minute interval following 2045 (74700) UT. Beginning at 2045 UT the number flux (JTOT) rises from 10^9 to 4×10^9 electrons/cm^2 sec sr at 2045:22 UT. In the next 20 sec

it decreased to 10^7 electrons/cm^2 sec sr. The average energy of the precipitating electrons increased from 800 eV to 7.5 keV then returned to 800 eV, the classic signature of an inverted-V structure. The flux of ions reaching the detector also increased to a sharp maximum at 2045:22 UT. However, the average energy of the ions was lowest at this time. This signature is similar to that obtained when spacecraft at geosynchronous orbit undergo charging.

Figures 4, 5 and 6 give three examples of measurements from the energetic electron and ion sensors at 2045:17, :22 and :24 UT, respectively. Data represented as electron and ion phase space densities are plotted as functions of energy from 30 eV to 30 keV. The insets give expanded plots of ion distribution functions in the energy range 30 to 200 eV. In all three cases the electron distributions show low-energy or suprathermal components. The fact that the energetic components of the electron distributions are not monotonically decreasing in energy is consistent with the primary electrons having been electrostatically accelerated in some attitude range above the satellite. Electrons with energies below the peak in the distribution functions are energy-degraded primaries that are trapped below the electrostatic barrier. The primary-electron distributions are non-Maxwellian, containing high energy tails.

The ion distribution functions also contain both energetic and suprathermal components. In the case of the ion measurement at 2045:22 UT the energetic component has a Maxwellian distribution out to 30 keV. Using the Liouville theorem and assuming an isotropic distribution function in the magnetosphere we find that for charge neutrality to prevail in the parent populations, the field-aligned potential drop above the auroral ionosphere is ~ 8 kV. We note that this is consistent with the measured distribution where the actual peak must lie between the energy channels centered at 6.46 and 9.48 keV.

At 20:45:22 and :24 UT the suprathermal ions have non-monotonic distributions. The peaks in the energy channels centered at 65 and 44 eV suggest that ions measured in these channels are ionospheric particles that have been accelerated by satellite potentials of -65 and -44 V, respectively. The fact that ion counts are recorded in energy channels less than at the peak in the distribution is consistent with the finite spread in the energy-acceptance of the sensor's energy channels. Recall that to assure high count rates the geometric factor of the low-energy ion detector was made large. The only other possible source of ions in these energy ranges at DMSP's altitude are the so-called ion conics (ref. 15). These are thermal ions that are accelerated perpendicular to magnetic field lines through resonant interactions with lower-hybrid or ion-cyclotron electrostatic waves. Such cannot be the case here since the ion detector is looking almost along, rather than across, the magnetic field. Note that the negative potentials of several tens of volts represent the potentials of the dielectric surfaces in the vicinity of the ion-detector's aperture rather than the potential of the satellite's frame.

Further information concerning the environment in which the charging of DMSP/F6 occurred can be gained from thermal probe measurements. Figure 7 gives the "densities" of thermal electrons and ions measured during Mode 1 operations. In this representation data taken while sensor grids were being swept in voltage (Mode 2) are suppressed. The grid on the spherical Langmuir probe was biased at 7.8 V with respect to the satellite frame. Thus, in Mode 1 the electron sensor is operating in the accelerating mode. This leads to overestimates of the ambient electron densities. In regions where both sensors vary in the same sense the measurements accurately measure relative density fluctuations. In regions where the measurements vary in

113

opposite senses the variations are mostly due to satellite potential fluctuations. Absolute values of the plasma density are obtained through analyses of Mode 2 current -voltage sweeps. Figure 7 shows that in the period following 2045 UT the current reaching the thermal electron probe decreased by more than four orders of magnitude, consistent with a strongly negative vehicle potential. The thermal ion current increased by a factor of 2.

In the immediate vicinity of the charging event Mode 2 sweeps cannot be used to determine the plasma temperature and composition. The last Mode 2 sweep, taken equatorward of the event and before vehicle potential fluctuations make results of Langmuire probe analysis questionable, occurred at 2043:26 UT. This sweep showed a total plasma density of $\sim 10^4 \mathrm{cm}^{-3}$. The ion composition was mostly O^+. The ion and electron temperatures were $\sim 1200°$ and 4000°K, respectively. The following sweep, beginning at 2044:30 UT showed signs of a significant light ion contribution. It should be noted that other measurements in the diffuse auroral region show large, even dominant light ion mixtures. The light ion that best fit the measured current-voltage characteristics was He^+. Close to the event the current characteristics also showed signs of a light-ion component. However, rapid fluctuations of the satellite potential do not allow quantitification of this observation.

DISCUSSION

In modelling the DMSP charging event described in the previous section two conditions should be kept in mind. First, the event occurred while the satellite was in darkness. Thus, photoemission currents from the vehicle can be ignored. Second, the surfaces of DMSP satellites are almost entirely made up of dielectric materials. The potential drop V_s experienced by positive ions reaching the electrostatic analyzer should be that required for local current balance near that sensor's aperture. For the sake of simplicity we model the satellite as a sphere whose surface material is kapton. The satellite moves at a speed of 7.4 km/s through the combined ionospheric and auroral plasmas.

The local current balance condition can be written in the form:

$$I(V) = -J_{eM} + J_{iM} + J_{e2} + J_{eB} + J_{ei} + J_{iI} = 0$$

The terms J_{eM} and J_{iM} represent currents due to energetic electrons and ions of magnetospheric origin, respectively. The energetic electrons include both primaries and energy degraded primaries. The terms J_{e2}, J_{eB}, and J_{ei} refer to currents generated by: (1) secondary electrons resulting from energetic electrons impacting the satellite, (2) backscattered energetic electrons, and (3) secondary electrons due to impacting ions, respectively. Currents resulting from impacting ionospheric ions are represented by J_{iI}.

If we assume that the auroral electrons are well approximated by an isotropic distribution function $f_{eM}(E)$ then the total currents to the satellite directly attributable to energetic electrons has the form

(2) $$J_e = J_{eo} \, e^{-qV_s/kT_e}$$

where $J_{eo} = -J_{eM} + J_{e2} + J_{eB}$; V_s is the satellite potential and q is the elementary (negative) unit of charge and $kT_e = 2/3 \langle E \rangle$. Here $\langle E \rangle$, the mean thermal energy of the energetic electrons is 5.45 keV. Finally,

$$(3) \quad J_{eo} = \frac{4\pi^2 q}{m^2} \int_0^\infty \int_0^{\pi/2} E\, f_{eM}(E) \left[1 - \Delta_2(E, \psi) - \Delta_B(E, \psi) \right]$$

$$\cdot \cos\psi \sin\psi\, d\psi\, dE$$

is the total current due to energetic electrons if the satellite were at plasma potential. The functions of energy and angle ψ from normal incidence, for secondary $[\Delta_2(E,\psi)]$ and backscattered $[\Delta_B(E,\psi)]$ electrons are given by Laframboise and co-workers (ref 16).

The current due to impacting ions can be represented in the form

$$(4) \quad J_i = J_{io}\left(1 + \frac{eV_s}{kT_i}\right)$$

where kT_i is the mean thermal energy of the magnetospheric ions. J_{io} represents the sum of $J_{iM} + J_{ei}$ if the satellite were at plasma potential

$$(5) \quad J_{io} = \frac{4\pi^2 e}{M_i} \int_0^\infty \int_0^{\pi/2} E\, f_{iM}(E) \left[1 + \Delta_{ei}(E, \psi) \right]$$

$$\cos\psi \sin\psi\, d\psi$$

$f_{iM}(E)$ is the distribution function of magnetospheric ions in the vicinity of the satellite. $\Delta_{ei}(E,\psi)$ is the secondary electron conversion factor (ref 16).

Values of J_{eo} and J_{io} in equations (3) and (5) were solved by numerical integration using the energetic electron and ion distribution functions measured at 2045: 22 UT. Setting V_s equal to -65 V in equations (2) and (4) and adding we calculate that in the vicinity of the ion sensor there is a current of 6.33 $\mu A/m^2$ flowing away from the satellite. From equation (1) we see that this must be balanced by the thermal ion current J_{iI} to the vehicle.

The current to the satellite due to ionospheric ions is given by a sum, over ion species α

$$(6) \quad J_{iI} = N_o e\, U_{sat} \sum_\alpha \Gamma_\alpha (b_\alpha, \Theta)$$

where N_0 is the total ion density, U_{sat} is the satellite speed, Θ is the angle with respect to the ram direction, b_α is the Mach number of the α species $[1/2\, M_\alpha V_s/kT_e]^{1/2}$. Based on satellite measurements in the ionosphere, Gurevich and co-workers (ref. 17) derived an expression for the angular term

$$(7) \quad \Gamma_\alpha(b_\alpha, \Theta) = \frac{N_\alpha}{N_0} \left[\frac{1 + erf(b_\alpha \cos\phi_0}{1 + erf(b_\alpha \cos\phi_0)} \cos\Theta \right]$$

where erf (x) represents the standard error function. ϕ_0 is the complement of

the Mach angle. With $U_{sat} = 7.4$ km/s and $T_{e^+} = 4000°$ K we calculate values of $\phi_0 = 71°$ for an O^+ plasma and $55°$ for an He^+ plasma. Note that for $\Theta = 0°$ $\sum\limits_{\alpha} \Gamma_\alpha = 1$ and the current $N_{oe} U_{sat}$ is the ram current. For a plasma density N_0 of 10^4 cm^{-3} the ram current is 11.8 $\mu A/m^2$. Thus, to balance a current of 6.33 $\mu A/m^2$, $\sum\limits_{\alpha} \Gamma_\alpha (90°)$ must equal 0.536.

Figure 8 is a plot of $\sum\limits_{\alpha} \Gamma_\alpha (90°)$ plotted as a function of the fraction of He^+ present in the ionospheric plasma. The horizontal line at 0.536 represents the value of $\sum\limits_{\alpha} \Gamma_\alpha (90°)$ required to balance the auroral current with $V_s = -65$ V on the top surface of the satellite. The solutions are not unique. As expected the $\phi_0 = 55°$ condition is satisfied only for a pure He^+ plasma. Higher values of ϕ_0 require less He^+.

It is interesting to now use this model to estimate the surface potential in the wake region of a small satellite like DMSP. To do this we first choose a value of ϕ_0 which gives a solution to $V_s = -65V$ at $\Theta = 90°$. This is equivalent to some mixture of He^+ and O^+. With this we next solve equation (6) for the ionospheric ion current at any location on the satellite. The final step is to solve equations (2) and (4) for the potential V_s that gives an $I(V) = 0$ solution to equation (1).

Figure 9 demonstrates the results of this procedure. Here we have chosen the value $\phi_0 = 60°$. From Figure 8 we see that this corresponds to a case with $N_{He^+}/N_0 = 0.63$. On the ram side of the vehicle the potential is slightly positive. As we go away from $90°$ into the wake direction the model predicts that the surface potential rises quickly and saturates at a value of ~ 1 kV. We have examined the model predictions for other values of ϕ_0 in the range $55°$ to $70°$ and found that within a few percent the results are insensitive to these variations.

REFERENCES

1. Mozer, F.S., Cattell, C.A., Hudson, M.K., Lysak, R.L., Temerin, M., and Torbert, R.B. (1980) Satellite measurements and theories of low altitude auroral particle acceleration, Sp. Sci. Rev. 27: 155.

2. Lin, C.S. and Hoffman, R.A. (1979) Characteristics of the inverted-V event, J. Geophys. Res. 84: 1514.

3. Frank, L.A. and Ackerson, K.L. (1971) Observation of charged particle precipitation into the auroral zone, J. Geophys. Res. 76: 3612.

4. Frank, L.A., and Ackerson, K.L., (1972) Local time survey of plasma at low altitudes over the auroral zone, J. Geophys. Res. 77: 4116.

5. Akasofu, S.-I. (1964) The development of the auroral substorm, Planet. Sp. Sci. 12: 273.

6. Akasofu, S.-I., Kimball, D.S. and Meng, C.-I. (1965) The dynamics of the aurora, II, Westward travelling surges, J. Atmos. Terr. Phys. 27: 173.

7. Meng, C.-I., Synder, A.L. and Kroehl, H.W. (1978) Observations of auroral westward travelling surges and electron precipitations, J. Geophys. Res. 83: 575.

8. Mullen, E.G., and Gussenhoven, M.S. (1982) High-level spacecraft charging environments near geosynchronous orbit, AFGL-TR-82-0063 Hanscom AFB, MA 01731.

9. Burch, J.L., Fields, S.A., Hanson, W.B., Helis, R.A., Hoffman, R.A. and Janetzke, R.W. (1976), Characteristics of auroral acceleration regions observed by Atmosphere Explorer C., J. Geophys. Res. 81: 2223.

10. Dandekar, B.S., and Pike, C.P. (1978) The midday, discrete auroral gap, J. Geophys. Res., 83: 4227.

11. Hardy, D.A. (1983) The worst case, charging environment, in Proceeding of AFGL Workshop on Natural Charging of Large Space-Structures in Near-Earth Polar Orbit: Sept 14-15, 1982, ed by R. C. Sagalyn, D.E. Donatelli and I. Michael AFGL-TR - 83-0046, Hanscom AFB, MA, 01731.

12. Burke, W. J. (1983) Environmental interactions of polar orbiting satellites, in Proceedings of AFGL Workshop on Natural Charging of Large Space-Structures in Near-Earth Polar Orbit: Sept. 14-15, 1982, ed. by R. C. Sagalyn, D. E. Donatelli and I. Michael, AFGL-TR-83-0046, Hanscom AFB, MA 01731.

13. Smiddy, M., Sagalyn, R.C., Sullivan, W. P., Wildman, P. J. L., Anderson, P. and Rich, F. (1978) The topside ionosphere plasma monitor (SSIE, for the Block 5D/ Flight 2 DMSP satellite, AFGL-TR-78-0071, Hanscom AFB, MA 01731.

14. Rich, F.J., Smiddy, M., Sagalyn, R.C., Burke, W.J., Anderson, P., Bredesen, S. and Sullivan, W. P. (1980). In-flight characteristics of the topside ionospheric monitor (SSIE) on the DMSP satellite Flight 2 and Flight 4, AFGL-TR-80-0152, Hanscom AFB, MA 01731.

15. Gorney, D.J., Clarke, A., Croley, D., Fennell, J. Luhmann, J. and Mizera, P. (1981). The distribution of ion beams and conics below 8000 km, J. Geophys. Res. 86: 83.

16. Laframboise, J.G., Godard, R., Kamitsuma, M. (1982) Multiple floating potentials, "threshold temperature" effects, and "barrier" effects in high-voltage charging of exposed surfaces on a spacecraft" in Proceedings of International Symposium on Spacecraft Materials in Space Environment, Toulouse France, 8-11 June 1982, Publications Branch ESD, Noordwijk, The Netherlands.

17. Gurevich, A.V., Pitaevskii, L.P. and Smirnova, V.V. (1969) Ionospheric aerodynamics Space Sci. Rev. 9: 805.
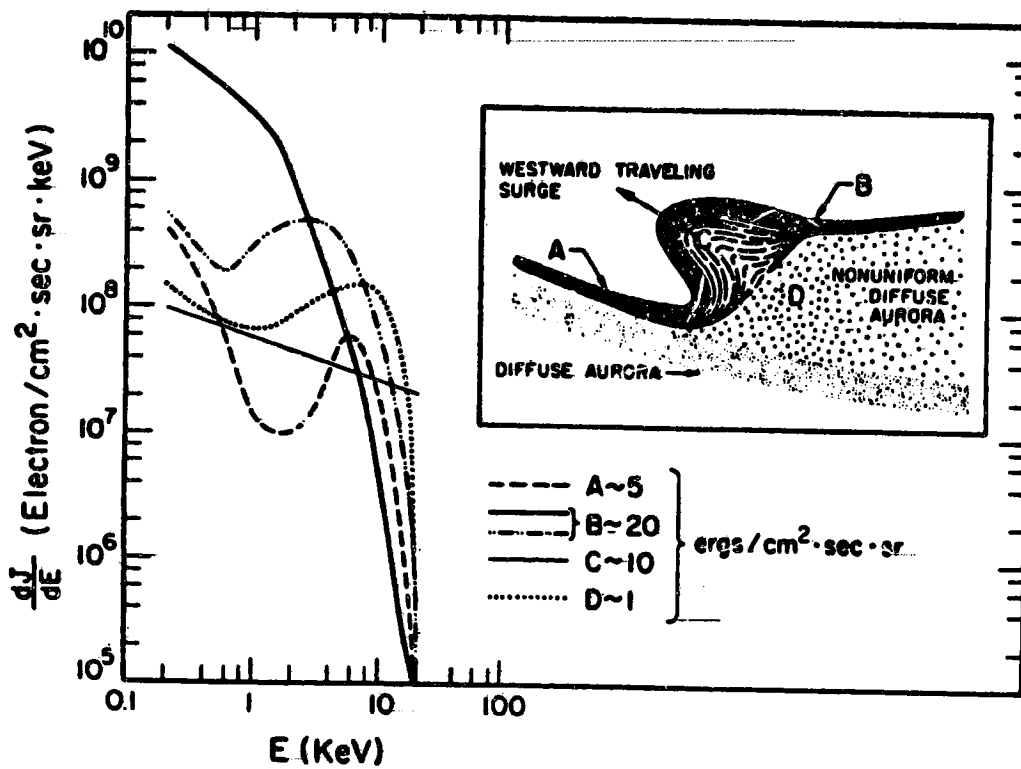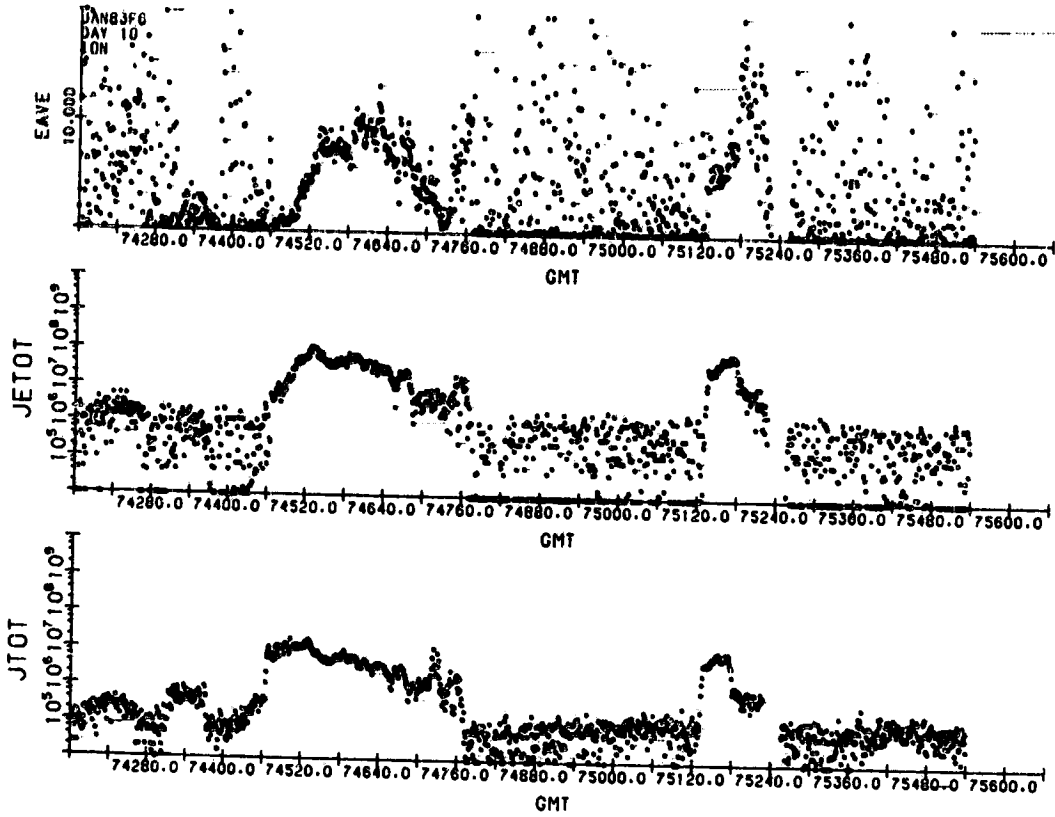
1. The morphology of auroral luminosity and precipitating electron spectra in the vicinity of westward travelling surges.
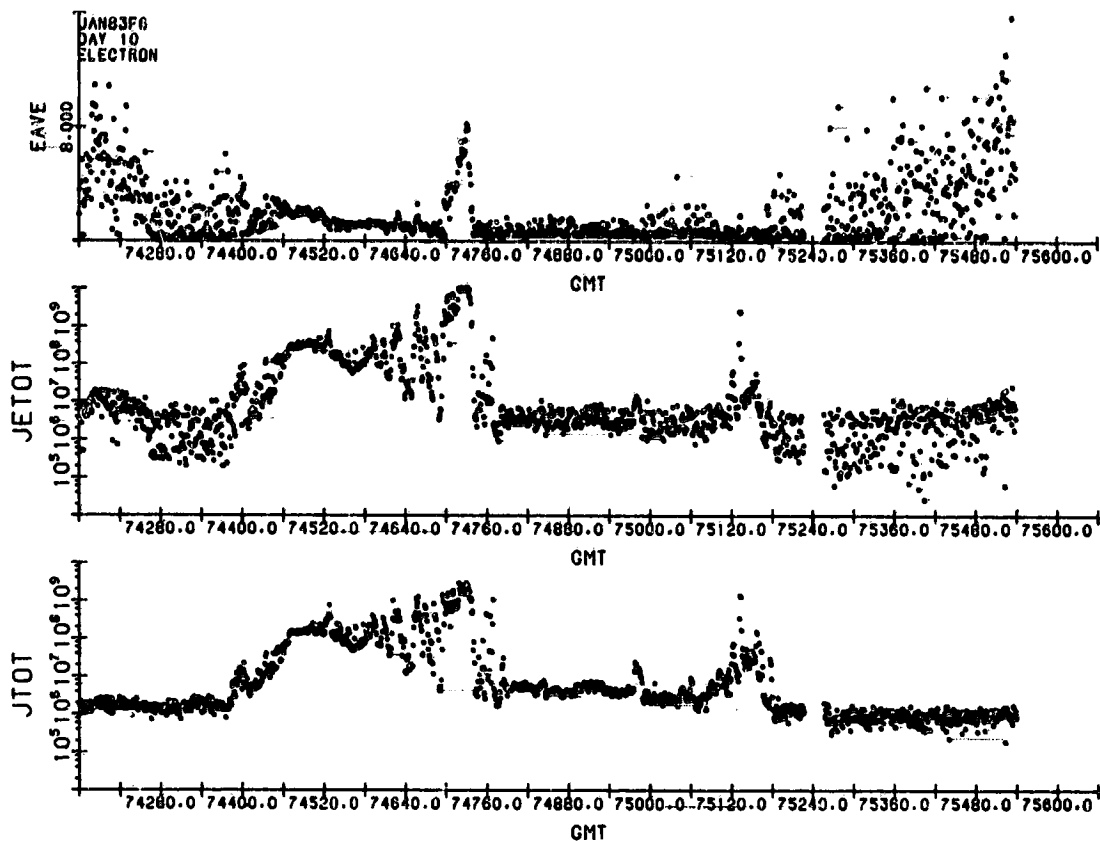
GLAT	61.3	67.9	74.1	79.3	81.2	78.2	72.7	66.4	59.7	52.9	46.0	0.0
GLON	127.5	121.0	109.9	87.6	46.4	9.0	350.3	340.7	334.9	330.9	327.8	0.0
MLAT	57.5	63.5	69.0	73.5	76.1	76.4	74.0	70.0	65.0	59.5	53.8	0.0
MLON	196.4	189.3	179.0	163.1	140.4	113.3	89.7	73.7	63.2	56.0	50.6	0.0
MLT	4.9	4.5	3.9	2.8	1.3	23.6	22.0	21.0	20.3	19.9	19.6	0.0

2. Average energy, directional energy flux and directional number flux of
pricipitating electrons measured during DMSP/F6 northern auroral pass of
10 January 1983.

119

CLAT	61.3	67.9	74.1	79.3	81.2	78.2	72.7	66.4	59.7	52.9	46.0	0.0
GLON	127.5	121.0	109.9	87.6	46.4	9.0	350.3	340.7	334.9	330.9	327.8	0.0
MLAT	57.5	63.5	69.0	73.5	76.1	76.4	74.0	70.0	65.0	59.5	53.8	0.0
MLON	196.4	189.3	179.0	163.1	140.4	113.3	89.7	73.7	63.2	59.5	50.6	0.0
MLT	4.9	4.5	3.9	2.8	1.3	23.6	22.0	21.0	20.3	19.9	19.6	0.0

3. Average energy, directional energy flux and directional number flux of downcoming ions measured during DMSP/F6 northern auroral pass of 10 January 1983.
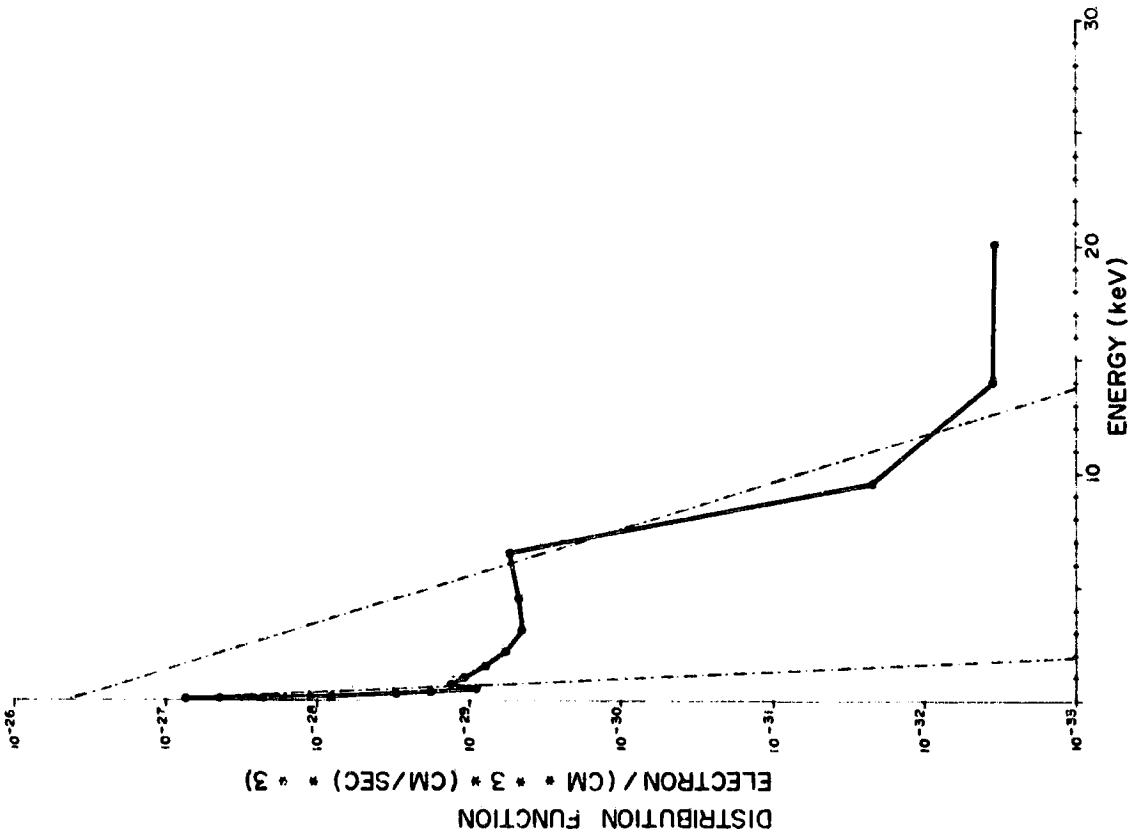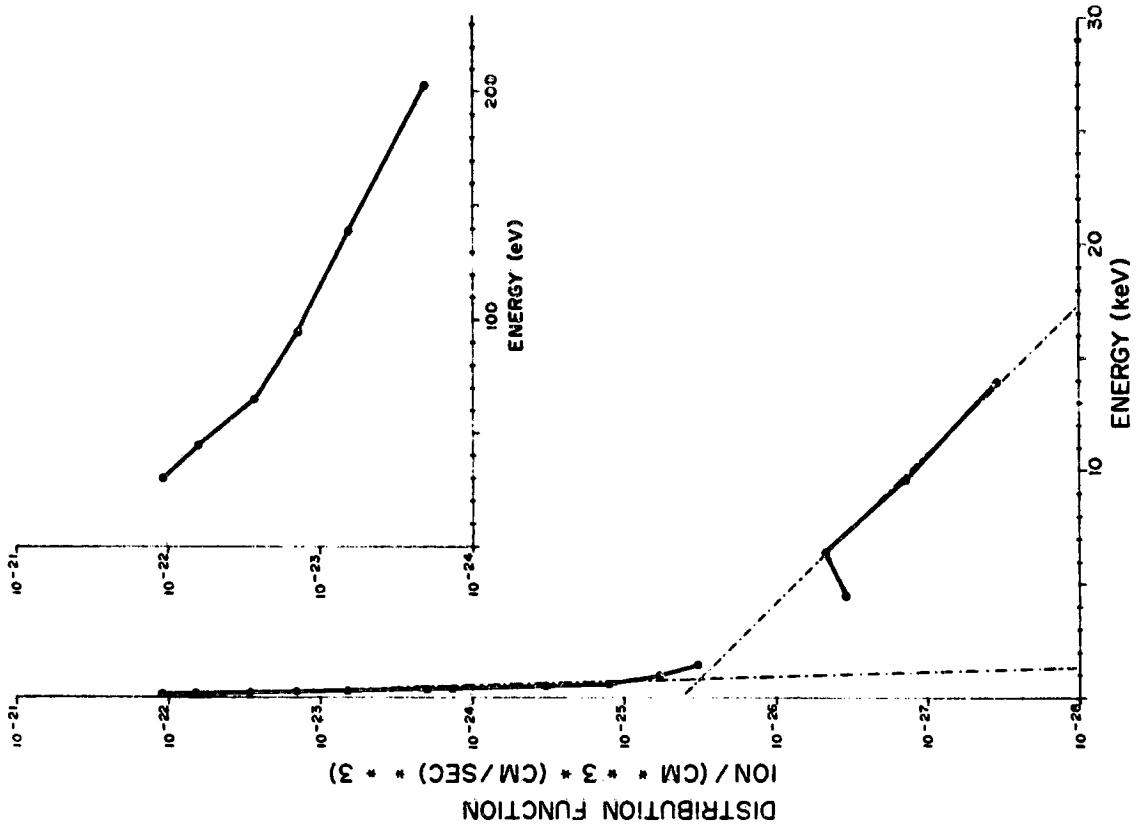
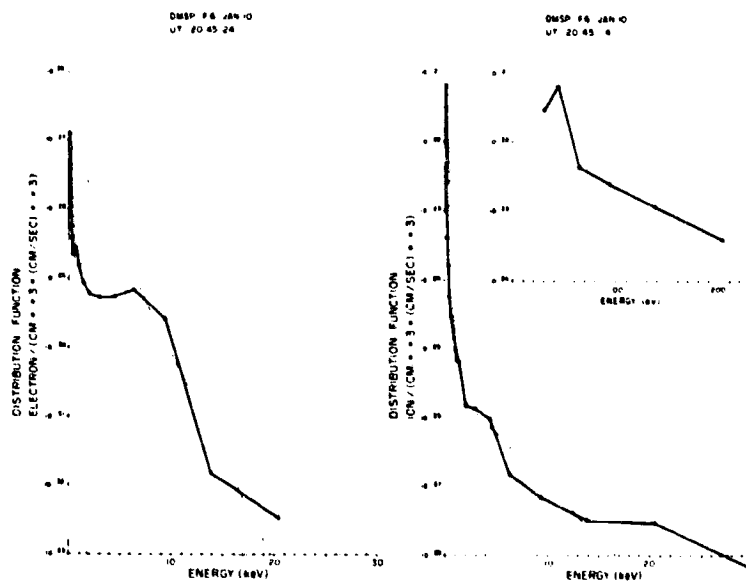4. Distribution functions of downcoming electrons and ions with energies between 30eV and 30 keV detected at 2045:17 UT of 10 January 1983.
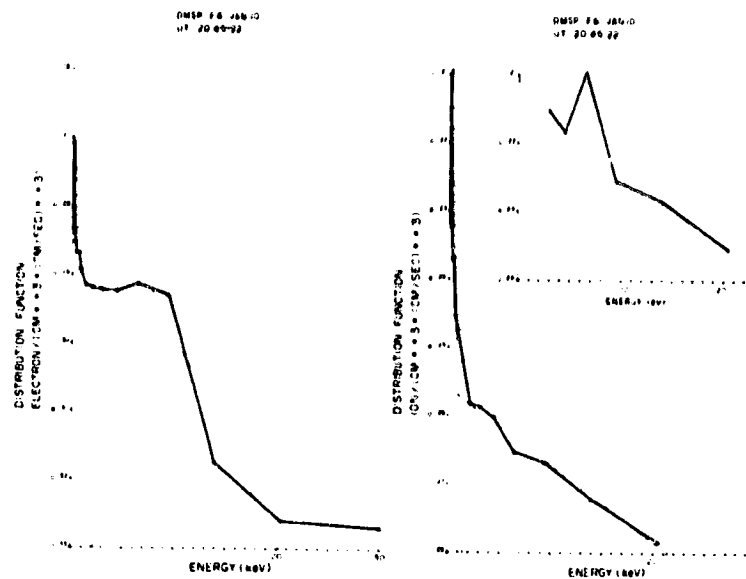
5. Distribution functions at 2045:22 UT in same format as Figure 4. The inset expansion of the low energy portion of ion distribution function shows a charging peak at 65 eV.


6. Distribution functions at 2045:24 UT, in same format as Figure 4. Here the charging peak is at 44 eV.
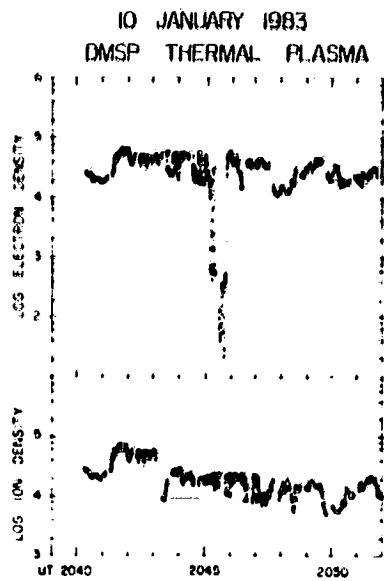
10 JANUARY 1983
DMSP THERMAL PLASMA

7. Mode 1 currents to the thermal electron and ion sensors during the northern auroral pass of 10 January. The "densities" calculated from these currents assume that the grids are at plasma potential and are overestimates in both cases.
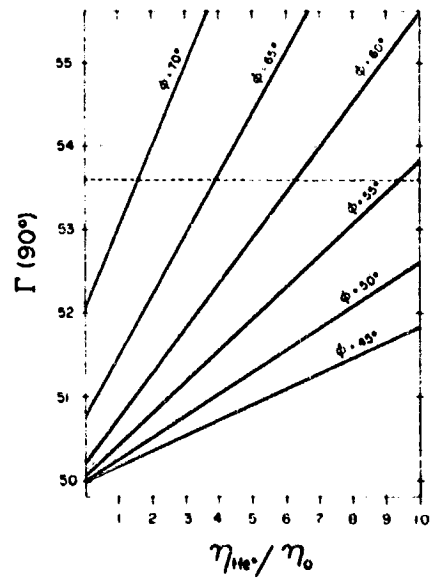
8. Plot of Γ, with θ set equal to 90°, as a function of $N_{H_e^+}/N_o$, for several values of ϕ_0. The line at 0.536 represents the value of Γ required for current balance with $V_S = -65$ V on the top surface of DMSP.
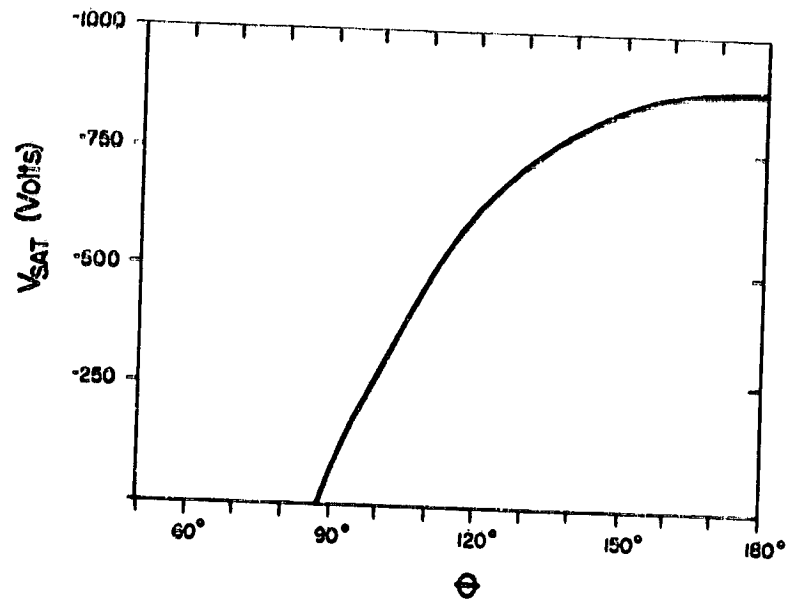
9. Surface potential as a function of 0 for $\phi_0 = 60°$.